Thyroid

DOI: 10.1089/thy.2019.0780

Nomogram based on shear-wave elastography radiomics can improve preoperative cervical lymph node staging for papillary thyroid carcinoma

Meng Jiang[1], MD, Ph.D, Changli Li[2], MD, Shichu Tang[3], MD, Wenzhi Lv[4], B.S., Aijiao Yi[5], MD, Bin Wang[5], MD, Ph. D, Songyuan Yu, MD[6], Xinwu Cui[1], MD, Ph.D, Christoph F. Dietrich[7], MD, Ph.D

[1]Department of Medical Ultrasound, Tongji Hospital, Tongji Medical College, Huazhong University of Science and Technology, 1095 Jiefang Road, Wuhan 430030, China

[2]Hubei Provincial Hospital of Integrated Chinese and Western medicine, 11 Lingjiaohu Avenue, Wuhan 430015, China

[3]Department of Medical Ultrasound, Hunan Cancer Hospital/The Affiliated Cancer Hospital of Xiangya School of Medicine, Central South University, Changsha, Hunan 410013, China

[4]Department of Artificial Intelligence, Julei Technology Company, Wuhan, 430030, China

[5]Department of Medical Ultrasound, The First People's Hospital of Yueyang, Yueyang, 414000, China

[6]Department of Medical Ultrasound, Shanghai Tenth People's Hospital, Ultrasound Research and Education Institute, Tongji University School of Medicine, Shanghai, China

[7]Department of Internal Medicine, Hirslanden Clinic, Schänzlihalde 11, 3013, Bern, Switzerland

Emails: Meng Jiang, jiangmenghust@163.com;

Changli Li, 1670244200@qq.com;

Shichu Tang, tsc163@163.com;

Wenzhi Lv, wenzhilv3@hotmail.com;

Aijiao Yi, 938186822@163.com;

Bin Wang, wangb58@mail2.sysu.edu.cn;

Songyuan Yu, 236770584@qq.com

Xinwu Cui, cuixinwu@live.cn;

Christoph F. Dietrich, christoph.dietrich@ckbm.de;

Meng Jiang and Chanli Li contributed equally to this study.

Running title: SWE radiomics nomogram for LN staging in PTC.

Keywords: Papillary thyroid carcinoma; lymph node metastasis; shear-wave elastography; radiomics; nomogram

Thyroid
Nomogram based on shear-wave elastography radiomics can improve preoperative cervical lymph node staging for papillary thyroid carcinoma (DOI: 10.1089/thy.2019.0780)
This paper has been peer-reviewed and accepted for publication, but has yet to undergo copyediting and proof correction. The final published version may differ from this proof.

Thyroid
Nomogram based on shear-wave elastography radiomics can improve preoperative cervical lymph node staging for papillary thyroid carcinoma (DOI: 10.1089/thy.2019.0780)
This paper has been peer-reviewed and accepted for publication, but has yet to undergo copyediting and proof correction. The final published version may differ from this proof.

Abstract

Background Accurate preoperative prediction of cervical lymph node (LN) metastasis in patients with papillary thyroid carcinoma (PTC) provide a basis for surgical decision making and the extent of tumor resection. This study aimed to develop and validate an ultrasound radiomics nomogram for the preoperative assessment of LN status.

Methods Data from 147 PTC patients at the Wuhan Tongji Hospital and 90 cases at the Hunan Provincial Tumor Hospital between January 2017 and September 2019 were included in our study. They were grouped as training and external validation set. Radiomics features were extracted from shear-wave elastography (SWE) images and corresponding B-mode ultrasound (BMUS) images. Then, the minimum redundancy maximum relevance (mRMR) algorithm and the least absolute shrinkage and selection operator (LASSO) regression were used to select LN status-related features and construct the SWE and BMUS radiomics score (Rad-score). Multivariate logistic regression was performed using the two radiomics scores together with clinical data, and a nomogram was subsequently developed. The performance of the nomogram was assessed with respect to discrimination, calibration, and clinical usefulness in the training and external validation set.

Results Both the SWE and BMUS Rad-scores were significantly higher in patients with cervical LN metastasis. Multivariate analysis indicated that SWE Rad-score, multifocality and US-reported LN status were independent risk factors associated with LN status. The radiomics nomogram, which incorporated the three variables showed good calibration and discrimination in the training set (AUC 0.851; 95% CI, 0.791-0.912) and the validation set (AUC 0.832; 95% CI, 0.749-0.916). The significantly improved net reclassification index (NRI) and integrated discriminatory improvement (IDI) demonstrated that SWE radiomics signature was a very useful marker to predict the LN metastasis in PTC. Decision curve analysis indicated that the SWE radiomics nomogram was clinically useful. Furthermore, the nomogram also showed favorable discriminatory efficacy in the US-reported LN negative (cN0) subgroup (AUC 0.812; 95% CI, 0.745-0.860).

Conclusion The presented radiomics nomogram, which is based on the SWE radiomics signature, shows favorable predictive value for LN staging in patients with PTC.

Thyroid
Nomogram based on shear-wave elastography radiomics can improve preoperative cervical lymph node staging for papillary thyroid carcinoma (DOI: 10.1089/thy.2019.0780)

Thyroid
Nomogram based on shear-wave elastography radiomics can improve preoperative cervical lymph node staging for papillary thyroid carcinoma (DOI: 10.1089/thy.2019.0780)
This paper has been peer-reviewed and accepted for publication, but has yet to undergo copyediting and proof correction. The final published version may differ from this proof.

Introduction

Papillary thyroid carcinoma (PTC) is the most common type of primary thyroid malignancy, with rapidly increasing incidence but stable high survival rate worldwide (1,2). Although PTC has an indolent clinical course, metastasis remains an important issue. PTC is a lymphotropic tumor where cervical lymph node (LN) metastasis is present at diagnosis in 20-90% of patients (3). Recent trends in the surgical treatment of PTC have changed to more individualized and conservative therapies, especially for small unifocal (<1 cm) tumors without extrathyroidal extension and LN metastasis (4). The revised American Thyroid Association (ATA) guidelines recommend that lobectomy alone can be used safely in patients with no LN metastasis (4). However, it remains difficult for clinicians to identify LN metastasis in clinical practice. Since cervical LN metastasis is an important risk factor for recurrence (5-11) and mortality (10,12-14) in PTC patients, its accurate preoperative identification will influence decisions about the extent of surgery.

B-mode ultrasound (BMUS) is the first-line noninvasive imaging method for preoperative assessment of cervical LN status for PTC, with high reported specificity (85.0%-97.4%) but relative low sensitivity (36.7%-61.0%) (15-18). Recently, several studies have explored the clinical utility of shear-wave elastography (SWE) in detecting tumor sonographic features associated with cervical LN metastasis (19-22). The results demonstrated that the quantitative elasticity index on preoperative SWE imaging could be useful for predicting LN metastasis.

Radiomics is the process of high-throughput mining of quantitative image features from medical imaging, which enables data to be extracted and applied in a clinical-decision support system to improve the diagnostic, predictive and prognostic accuracy (23). Radiomics derived data, when combined with other pertinent clinicopathological features, can produce accurate and robust evidence-based decision-making systems (24). Recently, radiomics characteristics of preoperative US images have been shown to have potential for predicting LN metastasis for PTC (25,26).

Nomogram is an individualized and evidence-based graphic tool for assessing the probability of a clinical event. It has been shown that nomograms incorporating clinical risk

factors, such as age, sex, number of positive LNs and tumor size, can be helpful in predicting LN metastasis for PTC, with area under the receiver operator characteristic (ROC) curve (AUC) ranging from 0.711 to 0.834 (3,27-29). To the best of our knowledge, there is no report that has determined whether a nomogram involving SWE radiomics features would enable superior prediction of cervical LN metastasis for PTC. Therefore, this study aimed to develop and validate a nomogram that incorporated the SWE radiomics as well as clinicopathological risk factors for individual preoperative prediction of cervical LN metastasis in PTC.

Materials and Methods

Patients

Between January 2017 and September 2019, consecutive patients with thyroid nodules in hospital #1 (Tongji Hospital of Huazhong University of Science and Technology, Wuhan, China, training cohort) and hospital #2 (Hunan Provincial Tumor Hospital, Changsha, China, validation cohort) were included. This retrospective study (clinical trial ChiCTR1900026179) was approved by the Institutional Review Board of the two hospitals, and informed consent was waived.

The study inclusion criteria were:1) surgical resection was performed for the target tumor; 2) the tumor was pathologically proven PTC; 3) SWE image of the tumor displayed with a BMUS image in split-screen mode was performed within two weeks prior to surgery; 4) the SWE images of the target tumor in the longest axis cross section were available; and 5) cervical LN dissection was performed and pathologically examined. The exclusion criteria included: 1） the pathological result of the surgical specimens was uncertain; 2) the patient had undergone preoperative radiofrequency ablation, radiotherapy or chemotherapy; 3) the target tumor was unclear on US images due to artifacts; 4) concomitant other malignancies.

The patients were divided into 2 groups (pN0 and pN1) according to the pathologic results of LN status after cervical LN dissection. In total, 147 patients were identified and comprise the training cohort (Wuhan cohort): 42 males and 105 females; mean age, 41.59

± 9.68 years; range, 22 to 67 years. An independent external validation cohort of 90 consecutive patients (Changsha cohort,16 males and 74 females; mean age, 43.14 ± 10.76 years; range, 23 to 66 years) was included using the same criteria.

Clinical information

Baseline clinicopathological data, including age, sex, and nodule pathology was derived from medical records and dates of US imaging were also recorded. The cutoff value for age were 45- and 55-year-old separately according to the 7th and 8th American Joint Committee on Cancer (AJCC) staging systems.

US image acquisition and reported LN status

BMUS and SWE images were acquired with a Supersonic Aixplorer system (SuperSonic Imagine, Aix en Provence, France) using a 5-14 MHz linear transducer by two radiologists with more than 10 years of experience. For the target tumor, the largest diameter was measured as tumor size on the BMUS image. The region of interest on SWE image was set to include the whole thyroid lesion and adjacent normal parenchyma, and a Q-Box was placed over the stiffest part of the lesion, as assessed by visual inspection. For mixed cystic and solid nodules, the Q-box was placed over the solid part of the lesion. More detailed descriptions on SWE was supplemented in the Appendix A1. We applied ACR TI-RADS system, which provides guidance regarding management of thyroid nodules on the basis of their BMUS appearance, for risk stratification (30). The results of SEW and color Doppler acted as auxiliary tool for further risk evaluation based on BMUS features. Fine-needle aspiration (FNA) biopsy was performed for suspected nodules prior to surgery, and the patients were handled based on the recommendations of 2015 ATA management guidelines for adult patients with thyroid nodules and differentiated thyroid cancer according to various cytologic categories (31).

The US-reported LN status was documented by the radiologists, and images containing important features of LNs were stored into the Picture Archiving and Communication Systems (PACS). It was retrospectively reviewed and verified by 2 radiologists (A.J.Y and S.Y.Y) with over 10 years of experience. Metastatic LNs were deemed present by US when at least one of the five criteria was met: 1) focal or diffuse hyperechogenicity, 2) micro- or

macrocalcification, 3) cystic change, 4) abnormal vascular pattern (a chaotic or peripheral vascular pattern), 5) or a round shape (long/transverse diameter ratio < 1.5) (15,17,32). One or more nodes that met at least one of the five US criteria would be considered as positive, regardless of the site of the LN. Preoperative biopsy was performed for high-suspicion nodes in all cases.

Surgical technique

All patients diagnosed with thyroid cancer underwent total thyroidectomy with routine bilateral central neck dissection since 2008 in the two centers, regardless of disease stage or tumor size. Additional lateral LN dissection was performed in patients who had clinically suspicious lateral LN metastasis confirmed by preoperative FNA or an intraoperative frozen biopsy.

Region of interest segmentation and radiomics feature extraction

Region of interest (ROI) was manually delineated on the BMUS image of the largest cross section using an open-source software (ITK-SNAP 3.8.0; http://www.itksnap.org). All the manual segmentations were conducted by two radiologists and one radiologist (twice) with >5 years of experience in thyroid oncologic imaging who were blinded from the final LN status (for interobserver and intraobserver reproducibility evaluation). Because the boundary of the tumor in SWE image was indefinite, the ROI of BMUS image was directly applied as a template to corresponding SWE image. Then the SWE image was segmented by an adaptive threshold algorithm automatically followed by a morphologic closing process. Since SWE image contained a SWE color elasticity layer and the corresponding B-model image, methods that reported in previous study were applied to extract the SWE information and build a purified grayscale SWE elasticity image (33). SWE and corresponding BMUS images were then exported as DICOM format. The textural, morphological, intensity, laws and wavelet features were extracted automatically by using an open-source software (Pyradiomics; http://pyradiomics.readthedocs.io/en/latest/index.html) (34). The interclass correlation coefficient (ICC) was used to assess the interobserver and intraobserver agreement of the feature extraction. An ICC that was greater than 0.80 was considered excellent.

Thyroid
Nomogram based on shear-wave elastography radiomics can improve preoperative cervical lymph node staging for papillary thyroid carcinoma (DOI: 10.1089/thy.2019.0780)

LN status-related feature selection and radiomics signature building

Spearman's correlation coefficient was applied to calculate the relevance and redundancy of the features. Redundant features with a Spearman's correlation coefficient ≥0.8 were eliminated. Then, the minimum redundancy maximum relevance (mRMR) algorithm was used to choose the remaining features. The least absolute shrinkage and selection operator (LASSO) logistic regression method using 10-fold cross-validation was applied after mRMR to select the most useful predictive LN status-related features from the training data set (35). Radiomics score (Rad-score) was generated using a linear combination of the selected features weighted by the LASSO algorithm. The formula for the SWE and BMUS Rad-scores were built using the respective selected features. Then the potential association of the Rad-scores with LN status was assessed in the training and validation cohort by using a Mann-Whitney U test.

Development of US radiomics nomogram

Univariate analyses, either Student's independent test (continuous variables) or a χ^2 test (categorical variables), were used to identify the clinicopathological risk factor associated with cervical LN metastasis. A multivariate logistic regression analysis incorporating the Rad-scores and the independent clinical variables was performed, using backward step-down selection procedure with a liberal $P< 0.05$ as the retention criteria to select the final predictors for cervical LN metastasis. Then an US radiomics nomogram was developed based on the multivariate analysis in the training cohort. For comparison, a clinical prediction model was developed using the independent clinical risk factors alone.

Performance of the US radiomics nomogram

Calibration of the US radiomics nomogram was evaluated using calibration curve and Hosmer-Lemeshow test (a nonsignificant test statistic implies that the model calibrates perfectly) (36). The discrimination performance of the nomogram was evaluated using the AUC. Then the performance of the nomogram was tested in the external validation cohort by calibration curve and AUC.

Clinical utility of the US radiomics nomogram

Decision curve analysis (DCA) was conducted to determine the clinical usefulness of the US radiomics nomogram by quantifying the net benefits at different threshold probabilities in the combined training and validation set (37). The improvement in the predictive accuracy of the US radiomics nomogram was evaluated by the index integrated discrimination improvement (IDI) and the net reclassification improvement (NRI).

For clinical use, the nomogram predicted probability (defined as Nomo-score in this study) of each patient were calculated according to the nomogram algorithm. Then the optimal cutoff value was determined by maximizing the Youden index. Performance of the optimal cutoff value of the Nomo-score was assessed by the ROC, as well as sensitivity, specificity, predictive values, and likelihood ratios.

Statistical Analysis

Delong test was used to compare different AUC. Statistical analyses were conducted with R software 3.6.1 and SPSS19.0 software (SPSS Inc., Chicago, IL). All the statistical significance levels were two-sided, with P value less than 0.05. The packages of R3.6.1 that were used (Appendix Table A1) and detailed descriptions of the LASSO and DCA algorithm are provided in the Supplement data (Appendix A2).

Results

Clinical characteristics

The study flowchart is shown in **Figure 1**. Patients' clinical and pathological characteristics in the training and validation cohorts are summarized in **Table 1 and Table 2**. Except for nodular goiter and US-reported LN status, there were no differences in the other clinicopathological characteristics between the two cohorts. LN metastasis patients (pN1) accounted for 51.0% (75/147) and 42.2% (38/90) of the training and validation cohorts, respectively, and there were no significant differences between them (P = 0.188). In total, 18.5% (23/124) of the patients without LN metastasis (pN0) were overstaged and 51.3% (58/113) of the patients with LN metastasis (pN1) were understaged according to US-reported LN status in our study.

Establishment of US radiomics signature

One image per nodule was used for analysis. For patients with more than one nodule, only the image of the largest one was applied. Three-hundred ten imaging features were extracted from each BMUS image. The BMUS features were reduced to 2 LN status-related features after mRMR and LASSO algorithm in the training cohort (**Appendix Figure A1 A and B**). Likewise, the 209 SWE features were reduced to 4 risk predictors by mRMR algorithm and LASSO regression in the training cohort (**Appendix Figure A1 C and D**). Favorable interobserver and intraobserver reproducibility of feature extraction were achieved, with intraobserver ICCs ranging from 0.823 to 0.901 and the interobserver ICCs ranging from 0.716 to 0.930. The BMUS and SWE Rad-score calculation formulas are presented in the Supplementary material (Appendix A3). The BMUS and SWE Rad-scores were much higher in the pN1 group in both the training and validation sets than that in the pN0 group (**Table 3**).

Development and performance of the radiomics nomogram

The SWE radiomics signature, multifocality, and US-reported LN status were identified as independent predictors of LN metastasis in PTC patients by a multivariate logistic regression model (**Table 4**). A SWE radiomics nomogram incorporating these three predictors was constructed (**Figure 2A**). **Figure 2B** shows the calibration curve of the nomogram. The calibration curve and Hosmer-Lemeshow test statistic (P=0.226) showed good calibration in the training cohort. An AUC of 0.851 (95% CI, 0.791-0.912) also showed good discrimination by the nomogram (**Table 4**). The favorable calibration of the SWE radiomics nomogram was also confirmed in the validation set (**Figure 2C**). The Hosmer-Lemeshow test yielded a P value of 0.225, and the AUC of the validation set was 0.832 (95% CI, 0.749-0.916). Thus, our nomogram performed well in both the training and external validation sets.

Comparison of the SWE radiomics nomogram with the clinical model

The predictive performance of the SWE radiomics nomogram was superior to that of the clinical model in both the training set (AUC 0.851 vs. 0.800, P=0.034) and validation set (AUC 0.832 vs. 0.783, P=0.048) **(Table 4**). The DCA for the SWE radiomics nomogram is

presented in **Appendix Figure A2** The DCA demonstrated that the SWE radiomics nomogram had a higher overall net benefit than clinical model and US-reported LN status alone when the threshold probability for a clinician or a patient range from 0 to 0.83, and the nomogram was more beneficial than either the treat-all or the treat-none strategy.

The utilization of the SWE Rad-score significantly improved the predictive value for cervical LN metastasis in terms of NRI and IDI compared to the prediction model incorporating only the independent clinical risk factors (**Table 5**).

Predicting LN metastasis based on the Nomo-score

The optimal cutoff value of the Nomo-score was determined to be 0.574. The discrimination and AUC for differentiating the presence of LN metastasis were 0.851 (0.791-0.912) in the training cohort (**Figure 3A and B**), and 0.832 (0.749-0.916) in the validation cohort, respectively (**Figure 3C and D**). The performance of the optimal cutoff value of the Nomo-score is summarized in **Table 6**.

We further assessed the discriminatory ability of the SWE radiomics nomogram in all 237 patients and in the US reported LN-negative (cN0) subgroup (n=159). The patients were divided into low- and high-risk subsets based on the optimal cutoff value of the Nomo-score (0.574). Notably, the high-risk group had a greater proportion of cervical LN metastasis in all patients (**Figure 4A**) and in the cN0 sub-cohort (**Figure 4C**). **Figure 4B** shows ROC analyses comparing the discriminatory performance of the nomogram to those of the clinical model and the US-reported LN status alone for all 237 patients. The SWE radiomics nomogram yielded the greatest AUC of 0.839 (95% CI, 0.789-0.889). The nomogram also showed favorable discriminatory efficacy in the cN0 subset (AUC 0.812; 95% CI, 0.745-0.860; **Figure 4D**).

Discussion

LN metastasis is one of the most important clinical features associated with local recurrence and distant metastasis (38). The overall survival and disease-free survival are negatively impacted by cervical LN metastasis (39). Previous reports revealed that cervical LN metastasis are associated with a higher rate of distant metastasis, 11.2-fold (40), and

disease-related mortality, 3-fold (39). Therefore, accurate preoperative prediction of LN status in patients with PTC is important for clinical decision-making.

In the 2015 ATA guidelines (31), either total thyroidectomy or lobectomy is considered to be a reasonable surgical strategy for PTC measuring 1-4 cm without extrathyroidal extension or clinically apparent LN metastasis on preoperative examination or imaging. However, total thyroidectomy and prophylactic cervical LN dissection has potential for more harm, which may increase the risk of hypoparathyroidism and nerve injury. For properly selected patients, the recurrence rates may be as low as 4% if treated with lobectomy alone. The accurate preoperative identification of cervical LN metastasis could improve the surgical outcomes and quality of life in patients with low-risk PTC. Nevertheless, it is difficult to identify patients who will benefit from lobectomy without prophylactic cervical LN dissection.

Preoperative neck US for cervical LNs plays an important role in deciding the extent of surgical resection, especially for determining the need for LN dissection. Unfortunately, the detection rate of cervical LN metastasis by US is unsatisfactory, especially for central neck lymph node metastasis (41). In our data, 113 tumors had LN metastasis, however, only 48.7% (55/113) of them were correctly reported as LN positive by US. Many previous studies have explored the association between cervical LN metastasis and tumor ultrasonic features. Guo et al found that tumor size, echogenicity and calcification were significantly associated with LN status (42). In addition, “wider-than-tall” shape and extrathyroidal extension were also indicators of LN metastasis (43). Although the US characteristics mentioned above are encouraging, the diagnostic accuracy is significantly affected by the expertise of the operator.

Radiomics has recently attracted the interest of many researchers for predicting the LN metastasis with quantitative medical image features. A nomogram incorporating CT radiomics, carcinoembryonic antigen status (CEA) and CT reported LN status reached a C-index of 0.736 for the preoperative prediction of LN metastasis in patients with colorectal cancer (24). Wu et al demonstrated that nomogram based on the CT radiomics signature showed a favorable predictive value for LN metastasis in bladder cancer (44). Recently, a

Thyroid
Nomogram based on shear-wave elastography radiomics can improve preoperative cervical lymph node staging for papillary thyroid carcinoma (DOI: 10.1089/thy.2019.0780)
This paper has been peer-reviewed and accepted for publication, but has yet to undergo copyediting and proof correction. The final published version may differ from this proof.

nomogram that incorporated radiomics signature from contrast enhanced CT images showed promise for the preoperative prediction of cervical LN metastasis in patients with PTC with an AUC of 0.867. However, using iodinated contrast agents for contrast-enhanced CT may delay radioactive iodine therapy in patients with PTC (45). Moreover, contrast-enhanced CT is costly and time consuming, has a risk of contrast allergy, which is inconvenient for routine screening.

Liu and colleagues proposed a radiomics method based on preoperative BMUS images for staging LN status, which demonstrated the feasibility of applying an US radiomics analysis in patients with PTC (25). Thus, we attempted to develop a US-based radiomics nomogram for the preoperative prediction of LN metastasis in patients with PTC. Multimodal US technology, containing different aspects of anatomical and biological information about a tumor, has been applied conjointly for the diagnosis of thyroid tumors in clinical practice. Here, we investigated the value of SWE combined with BMUS for the prediction of LN metastasis using radiomics analysis. Interestingly, for univariate analysis, the BMUS and SWE radiomics signature were both significantly associated with LN status. However, BMUS Rad-score was not included in the final nomogram. We found that the strong discriminatory power of the SWE Rad-score diminished the value of BMUS radiomics signature in the final multivariate logistic regression analysis.

SWE is an elastographic technique used to evaluate the tissue hardness quantitatively. Several studies have shown that a higher elasticity index on SWE can be a sign of cervical LN metastasis for PTC (19,21). Radiomics analysis of SWE have been shown useful to distinguish benign and malignant thyroid nodules (33). However, to the best of our knowledge, no studies have investigated the association between the SWE radiomics features and LN status in PTC. In our study, the SWE radiomics signature showed favorable discrimination for LN status, yielding an AUC of 0.829 across all 237 patients. Our results demonstrated that radiomics analysis using SWE to predict cervical LN metastasis in patients with PTC can attain a satisfactory discriminatory efficacy. However, the relationship between thyroid cancer stiffness and the likelihood of LN metastasis remains to be elucidated. Many investigators have demonstrated that extracellular matrix cross-linking is an important ingredient of cancer cell biology and related to tissue stiffening in

Thyroid
Nomogram based on shear-wave elastography radiomics can improve preoperative cervical lymph node staging for papillary thyroid carcinoma (DOI: 10.1089/thy.2019.0780)
This paper has been peer-reviewed and accepted for publication, but has yet to undergo copyediting and proof correction. The final published version may differ from this proof.

tissue fibrosis (46,47). Tissue fibrosis influences tumor progression by regulating soluble factors that trigger inflammation and angiogenesis and induce cell growth and invasion (48). Therefore, it was speculated that tumor progression with cell proliferation and fibrosis could affect both tumor stiffness and aggressiveness including the development of regional LN metastasis (19).

We considered clinicopathological risk factors. A multivariate logistic regression analysis indicated that multifocality and US-reported LN status were significant predictive variables distinct from the SWE radiomics signature. To provide an easy-to-use tool for clinical use, we developed a radiomics nomogram based on the multivariate logistic regression analysis. Our nomogram exhibited good discrimination and calibration in the training and validation sets. The AUC of the nomogram was 0.851 in the training set and achieved greater predictive efficacy than the prediction model involving the clinical risk factors alone. The addition of SWE radiomics features to the clinical model significantly improved the NRI and IDI, implied that SWE radiomics signature could be a very useful new marker for staging LN status in PTC. DCA demonstrated that the SWE radiomics nomogram can improve patient LN staging preoperatively.

When categorized into low- and high-risk sub-cohorts according to the optimal cutoff value of the Nomo-score, the high-risk set have a significantly greater probability of cervical LN metastasis. Notably, our nomogram showed good discriminatory ability in the cN0 patients. PTC diagnosed as cN0 are considered to be at low risk of cervical LN metastasis. However, some cN0 patients may be understaged and actually harbor LN metastasis. Encouragingly, our nomogram showed good discrimination among these patients. Therefore, our SWE radiomics nomogram may serve as a reliable predictive tool for cervical LN metastases in patients with PTC.

For clinical use of the nomogram, we summarized the sensitivity, specificity, positive predictive value as well as negative predictive value in assessing the risk of LN metastasis. We show that patients with a Nomo-score of 0.574 or more are the subset of high-risk PTC likely to have cervical LN metastasis (positive predictive value, 79.25%). Thus, this subgroup of PTC patients may benefit from prophylactic cervical LN dissection. Since the

current nomogram was constructed regardless of the location of the metastatic LNs, it is appropriate to recommend that a high-risk score should prompt a central LN dissection, leaving the decision to perform a lateral LN dissection to be based on intraoperative findings.

Some limitations of our study should be acknowledged. First, some bias may inevitably exist and affect our analysis because it was a retrospective study. Prospective multicenter validation using a larger group of patients is needed to acquire high-level evidence for further clinical application. Second, since we performed routine bilateral central neck dissection for all patients, but additional lateral LN dissection was conducted based on preoperative FNA or an intraoperative frozen biopsy, the different strategy for LN dissection might be another source of bias. Third, although our nomogram showed favorable discriminatory ability in regard to negative predictive value and positive predictive value in the training and validation cohort, physicians might still encounter a dilemma in the case that non-aggressive-appearing primary tumors (e.g., no gross extrathyroidal extension) with cN0 PTCs were categorized as high risk of LN metastasis based on the nomogram and vice versa. In a situation like this, intra-operative evaluation of minimal or gross extrathyroidal extension might provide additional information for decision-making. Fourth, due to the lack of data on the size of the pathologically proven LNs, we could not determine if the nomogram was capable of detecting small as well as large nodal metastases, which necessitates a prospective cohort study in the future. In addition, genomic characteristics were not incorporated into our nomogram. In recent years, for preoperative nodal staging, the *BRAF*^{V600E} mutation in patients with PTC has been associated with a higher rate of LN metastasis (49,50). Radiogenomics consisting of a radiomics signature and gene marker may improve the ability for preoperative LN staging in patients with PTC.

In conclusion, this study presents a non-invasive predictive tool that incorporates both the SWE radiomics signature and clinical risk factors, shows favorable predictive accuracy in predicting preoperative cervical LN metastasis in patients with PTC.

Thyroid
Nomogram based on shear-wave elastography radiomics can improve preoperative cervical lymph node staging for papillary thyroid carcinoma (DOI: 10.1089/thy.2019.0780)
This paper has been peer-reviewed and accepted for publication, but has yet to undergo copyediting and proof correction. The final published version may differ from this proof.

Acknowledgements

This research was supported by grant from Wuhan Tongji Hospital (No. 2017A002), grant from Wuhan Science and Technology Bureau (No. 2017060201010181), Key project supported by the Xinjiang Construction Corps (2019DB012), and Project supported by the Health Commission of Hubei province (WJ2019H227).

Author Disclosure Statement

The authors have no relevant conflicts of interest to disclose.

Corresponding author: Xin-Wu Cui, MD, Ph.D, Sino-German Tongji-Caritas Research Center of Ultrasound in Medicine, Department of Medical Ultrasound, Tongji Hospital, Tongji Medical College, Huazhong University of Science and Technology, No. 1095, Jiefang Avenue, Wuhan 430030, Hubei Province, China.

Email: cuixinwu@live.cn

Thyroid
Nomogram based on shear-wave elastography radiomics can improve preoperative cervical lymph node staging for papillary thyroid carcinoma (DOI: 10.1089/thy.2019.0780)
This paper has been peer-reviewed and accepted for publication, but has yet to undergo copyediting and proof correction. The final published version may differ from this proof.

References:

1. Miller KD, Nogueira L, Mariotto AB, Rowland JH, Yabroff KR, Alfano CM, Jemal A, Kramer JL, Siegel RL 2019 Cancer treatment and survivorship statistics, 2019. CA Cancer J Clin **69**:363-385.

2. Siegel R, Ma J, Zou Z, Jemal A 2014 Cancer statistics, 2014. CA Cancer J Clin **64**:9-29.

3. Kim SK, Chai YJ, Park I, Woo J, Lee JH, Lee KE, Choe J, Kim J, Kim JS 2017 Nomogram for predicting central node metastasis in papillary thyroid carcinoma. J Surg Oncol **115**:266-272.

4. Cooper DS, Doherty GM, Haugen BR, Kloos RT, Lee SL, Mandel SJ, Mazzaferri EL, McIver B, Pacini F, Schlumberger M, Sherman SI, Steward DL, Tuttle RM 2009 Revised American Thyroid Association management guidelines for patients with thyroid nodules and differentiated thyroid cancer. Thyroid **19**:1167-1214.

5. Suh YJ, Kwon H, Kim SJ, Choi JY, Lee KE, Park YJ, Park DJ, Youn YK 2015 Factors Affecting the Locoregional Recurrence of Conventional Papillary Thyroid Carcinoma After Surgery: A Retrospective Analysis of 3381 Patients. Ann Surg Oncol **22**:3543-3549.

6. Kim TY, Hong SJ, Kim JM, Kim WG, Gong G, Ryu JS, Kim WB, Yun SC, Shong YK 2008 Prognostic parameters for recurrence of papillary thyroid microcarcinoma. Bmc Cancer **8**:296.

7. Baek SK, Jung KY, Kang SM, Kwon SY, Woo JS, Cho SH, Chung EJ 2010 Clinical risk factors associated with cervical lymph node recurrence in papillary thyroid carcinoma. Thyroid **20**:147-152.

8. Ito Y, Kudo T, Kobayashi K, Miya A, Ichihara K, Miyauchi A 2012 Prognostic factors for recurrence of papillary thyroid carcinoma in the lymph nodes, lung, and bone: analysis of 5,768 patients with average 10-year follow-up. World J Surg **36**:1274-1278.

9. Kruijff S, Petersen JF, Chen P, Aniss AM, Clifton-Bligh RJ, Sidhu SB, Delbridge LW, Gill AJ, Learoyd D, Sywak MS 2014 Patterns of structural recurrence in papillary thyroid cancer. World J Surg **38**:653-659.

10. Grogan RH, Kaplan SP, Cao H, Weiss RE, Degroot LJ, Simon CA, Embia OM, Angelos P, Kaplan EL, Schechter RB 2013 A study of recurrence and death from papillary thyroid cancer with 27 years of median follow-up. Surgery **154**:1436-1447.

11. Schneider DF, Mazeh H, Chen H, Sippel RS 2013 Lymph Node Ratio Predicts Recurrence in Papillary Thyroid Cancer. The Oncologist **18**:157-162.

12. Podnos YD, Smith D, Wagman LD, Ellenhorn JD 2005 The implication of lymph node metastasis on survival in patients with well-differentiated thyroid cancer. Am Surg **71**:731-734.

13. Zaydfudim V, Feurer ID, Griffin MR, Phay JE 2008 The impact of lymph node involvement on survival in patients with papillary and follicular thyroid carcinoma. Surgery **144**:1070-1078.

14. Adam MA, Pura J, Goffredo P, Dinan MA, Reed SD, Scheri RP, Hyslop T, Roman SA, Sosa JA 2015 Presence and Number of Lymph Node Metastases Are Associated With Compromised Survival for Patients Younger Than Age 45 Years With Papillary Thyroid Cancer. J Clin Oncol **33**:2370-2375.

15. Kim E, Park JS, Son KR, Kim JH, Jeon SJ, Na DG 2008 Preoperative diagnosis of cervical metastatic lymph nodes in papillary thyroid carcinoma: comparison of ultrasound, computed tomography, and combined ultrasound with computed tomography. Thyroid **18**:411-418.

16. Jeong HS, Baek CH, Son YI, Choi JY, Kim HJ, Ko YH, Chung JH, Baek HJ 2006 Integrated 18F-FDG PET/CT for the initial evaluation of cervical node level of patients with papillary thyroid carcinoma: comparison with ultrasound and contrast-enhanced CT. Clin Endocrinol (Oxf) **65**:402-407.

17. Choi JS, Kim J, Kwak JY, Kim MJ, Chang HS, Kim EK 2009 Preoperative staging of papillary thyroid carcinoma: comparison of ultrasound imaging and CT. AJR Am J Roentgenol **193**:871-878.

18. Roh JL, Park JY, Kim JM, Song CJ 2009 Use of preoperative ultrasonography as guidance for neck dissection in patients with papillary thyroid carcinoma. J Surg Oncol **99**:28-31.

19. Park AY, Kim J, Son EJ, Youk JH 2016 Shear-Wave Elastography for Papillary Thyroid Carcinoma can Improve Prediction of Cervical Lymph Node Metastasis. Ann Surg Oncol **23**:722-729.

20. Park YJ, Kim JA, Son EJ, Youk JH, Park CS 2013 Quantitative shear wave elastography as a prognostic implication of papillary thyroid carcinoma (PTC): elasticity index can predict extrathyroidal extension (ETE). Ann Surg Oncol **20**:2765-2771.

21. Jung WS, Kim JA, Son EJ, Youk JH, Park CS 2015 Shear wave elastography in evaluation of cervical lymph node metastasis of papillary thyroid carcinoma: elasticity index as a prognostic implication. Ann Surg Oncol **22**:111-116.

22. Cosgrove D, Barr R, Bojunga J, Cantisani V, Chammas MC, Dighe M, Vinayak S, Xu JM, Dietrich CF 2017 WFUMB Guidelines and Recommendations on the Clinical Use of Ultrasound Elastography: Part 4. Thyroid. Ultrasound Med Biol **43**:4-26.

23. Lambin P, Leijenaar R, Deist TM, Peerlings J, de Jong E, van Timmeren J, Sanduleanu S, Larue R, Even A, Jochems A, van Wijk Y, Woodruff H, van Soest J, Lustberg T, Roelofs E, van Elmpt W, Dekker A, Mottaghy FM, Wildberger JE, Walsh S 2017 Radiomics: the bridge between medical imaging and personalized medicine. Nat Rev Clin Oncol **14**:749-762.

24. Huang Y, Liang C, He L, Tian J, Liang C, Chen X, Ma Z, Liu Z 2016 Development and Validation of a Radiomics Nomogram for Preoperative Prediction of Lymph Node Metastasis in Colorectal Cancer. J Clin Oncol **34**:2157-2164.

25. Liu T, Zhou S, Yu J, Guo Y, Wang Y, Zhou J, Chang C 2019 Prediction of Lymph Node Metastasis in Patients With Papillary Thyroid Carcinoma: A Radiomics Method Based on Preoperative Ultrasound Images. Technol Cancer Res Treat **18**:1-13.

26. Liu T, Ge X, Yu J, Guo Y, Wang Y, Wang W, Cui L 2018 Comparison of the application of B-mode and strain elastography ultrasound in the estimation of lymph node metastasis of

papillary thyroid carcinoma based on a radiomics approach. Int J Comput Ass Rad **13**:1617-1627.

27. Wang Y, Guan Q, Xiang J 2018 Nomogram for predicting central lymph node metastasis in papillary thyroid microcarcinoma: A retrospective cohort study of 8668 patients. Int J Surg **55**:98-102.

28. Hei H, Song Y, Qin J 2016 A nomogram predicting contralateral central neck lymph node metastasis for papillary thyroid carcinoma. J Surg Oncol **114**:703-707.

29. Thompson AM, Turner RM, Hayen A, Aniss A, Jalaty S, Learoyd DL, Sidhu S, Delbridge L, Yeh MW, Clifton-Bligh R, Sywak M 2014 A Preoperative Nomogram for the Prediction of Ipsilateral Central Compartment Lymph Node Metastases in Papillary Thyroid Cancer. Thyroid **24**:675-682.

30. Tessler FN, Middleton WD, Grant EG, Hoang JK, Berland LL, Teefey SA, Cronan JJ, Beland MD, Desser TS, Frates MC, Hammers LW, Hamper UM, Langer JE, Reading CC, Scoutt LM, Stavros AT 2017 ACR Thyroid Imaging, Reporting and Data System (TI-RADS): White Paper of the ACR TI-RADS Committee. J Am Coll Radiol **14**:587-595.

31. Haugen BR, Alexander EK, Bible KC, Doherty GM, Mandel SJ, Nikiforov YE, Pacini F, Randolph GW, Sawka AM, Schlumberger M, Schuff KG, Sherman SI, Sosa JA, Steward DL, Tuttle RM, Wartofsky L 2016 2015 American Thyroid Association Management Guidelines for Adult Patients with Thyroid Nodules and Differentiated Thyroid Cancer: The American Thyroid Association Guidelines Task Force on Thyroid Nodules and Differentiated Thyroid Cancer. Thyroid **26**:1-133.

32. Lu W, Zhong L, Dong D, Fang M, Dai Q, Leng S, Zhang L, Sun W, Tian J, Zheng J, Jin Y 2019 Radiomic analysis for preoperative prediction of cervical lymph node metastasis in patients with papillary thyroid carcinoma. Eur J Radiol **118**:231-238.

33. Bhatia KSS, Lam ACL, Pang SWA, Wang D, Ahuja AT 2016 Feasibility Study of Texture Analysis Using Ultrasound Shear Wave Elastography to Predict Malignancy in Thyroid Nodules. Ultrasound in Medicine & Biology **42**:1671-1680.

34. van Griethuysen J, Fedorov A, Parmar C, Hosny A, Aucoin N, Narayan V, Beets-Tan R, Fillion-Robin JC, Pieper S, Aerts H 2017 Computational Radiomics System to Decode the Radiographic Phenotype. Cancer Res **77**:e104-e107.

35. Sauerbrei W, Royston P, Binder H 2007 Selection of important variables and determination of functional form for continuous predictors in multivariable model building. Stat Med **26**:5512-5528.

36. Kramer AA, Zimmerman JE 2007 Assessing the calibration of mortality benchmarks in critical care: The Hosmer-Lemeshow test revisited. Crit Care Med **35**:2052-2056.

37. Fitzgerald M, Saville BR, Lewis RJ 2015 Decision curve analysis. JAMA **313**:409-410.

38. Zhao Q, Ming J, Liu C, Shi L, Xu X, Nie X, Huang T 2013 Multifocality and Total Tumor Diameter Predict Central Neck Lymph Node Metastases in Papillary Thyroid Microcarcinoma. Ann Surg Oncol **20**:746-752.

39. Lundgren CI, Hall P, Dickman PW, Zedenius J 2006 Clinically significant prognostic factors for differentiated thyroid carcinoma. Cancer-Am Cancer Soc **106**:524-531.

40. Chow S, Law SCK, Chan JKC, Au S, Yau S, Lau W 2003 Papillary microcarcinoma of the thyroid?Prognostic significance of lymph node metastasis and multifocality. Cancer-Am Cancer Soc **98**:31-40.

41. Xu SY, Yao JJ, Zhou W, Chen L, Zhan WW 2019 Clinical characteristics and ultrasonographic features for predicting central lymph node metastasis in clinically node-negative papillary thyroid carcinoma without capsule invasion. Head & Neck **41**:3984-3991.

42. Guo L, Ma Y, Yao Y, Wu M, Deng Z, Zhu F, Luo Y, Tang J 2019 Role of ultrasonographic features and quantified BRAFV600E mutation in lymph node metastasis in Chinese patients with papillary thyroid carcinoma. Sci Rep **9**:1-9.

43. Wang QC, Cheng W, Wen X, Li JB, Jing H, Nie CL 2014 Shorter distance between the nodule and capsule has greater risk of cervical lymph node metastasis in papillary thyroid carcinoma. Asian Pac J Cancer Prev **15**:855-860.

44. Wu S, Zheng J, Li Y, Yu H, Shi S, Xie W, Liu H, Su Y, Huang J, Lin T 2017 A Radiomics Nomogram for the Preoperative Prediction of Lymph Node Metastasis in Bladder Cancer. Clin Cancer Res **23**:6904-6911.

45. R.J. Amdur, E.L. Mazzaferri 2005 Intravenous iodinated contrast effects iodine 511 uptake for months, in: R.J. Amdur, E.L. Mazzaferri (Eds.), Essentials of Thyroid Cancer Management. 1st edition. Springer, New York, pp 211–213.

46. Lu P, Weaver VM, Werb Z 2012 The extracellular matrix: A dynamic niche in cancer progression. The Journal of Cell Biology **196**:395-406.

47. Levental KR, Yu H, Kass L, Lakins JN, Egeblad M, Erler JT, Fong SF, Csiszar K, Giaccia A, Weninger W, Yamauchi M, Gasser DL, Weaver VM 2009 Matrix crosslinking forces tumor progression by enhancing integrin signaling. Cell **139**:891-906.

48. Bierie B, Chung CH, Parker JS, Stover DG, Cheng N, Chytil A, Aakre M, Shyr Y, Moses HL 2009 Abrogation of TGF-beta signaling enhances chemokine production and correlates with prognosis in human breast cancer. The Journal of clinical investigation **119**:1571-1582.

49. Xing M 2007 BRAF mutation in papillary thyroid cancer: pathogenic role, molecular bases, and clinical implications. Endocr Rev **28**:742-762.

50. Chen J, Li X, Zhao C, Wang D, Wang Q, Li M, Wei Q, Ji G, Xu H 2018 Conventional Ultrasound, Immunohistochemical Factors and BRAFV600E Mutation in Predicting Central Cervical Lymph Node Metastasis of Papillary Thyroid Carcinoma. Ultrasound in Medicine & Biology **44**:2296-2306.

Table 1. Clinical characteristics of patients in the training and validation cohorts.

Characteristic	Training cohort (n=147)	Validation cohort (n=90)	P-value
Age, mean ± SD, years	41.59 ± 9.68	43.14 ± 10.76	0.250
Age (years)			0.140
>55	11 (7.5)	12 (13.3)	
≤55	136 (92.5)	78 (86.7)	
Age (years)			0.376
>45	52 (35.4)	37 (41.1)	
≤45	95 (64.6)	53 (58.9)	
LN metastasis			0.188
Positive	75 (51.0)	38 (42.2)	
Negative	72 (49.0)	52 (57.8)	
Gender			0.061
Male	42 (28.6)	16 (17.8)	
Female	105 (71.4)	74 (82.2)	
Primary site			0.727
Right lobe	69 (46.9)	47 (52.2)	
Left lobe	74 (50.3)	41 (45.6)	
Isthmus	4 (2.7)	2 (2.2)	
Tumor location			0.872
Subcapsular thyroid	62 (42.2)	37 (41.1)	
Intra-thyroidal	85 (57.8)	53 (58.9)	
Tumor size, mean ± SD, mm	12.46 ± 7.40	11.64 ± 5.77	0.347
*Multifocality			0.779
Positive	32 (21.8)	21 (23.3)	
Negative	115 (78.2)	69 (76.7)	
US-reported LN status			<0.001
Positive	32 (21.8)	46 (51.1)	
Negative	115 (78.2)	44 (48.9)	

Thyroid
Nomogram based on shear-wave elastography radiomics can improve preoperative cervical lymph node staging for papillary thyroid carcinoma (DOI: 10.1089/thy.2019.0780)
This paper has been peer-reviewed and accepted for publication, but has yet to undergo copyediting and proof correction. The final published version may differ from this proof.

Thyroid
Nomogram based on shear-wave elastography radiomics can improve preoperative cervical lymph node staging for papillary thyroid carcinoma (DOI: 10.1089/thy.2019.0780)
This paper has been peer-reviewed and accepted for publication, but has yet to undergo copyediting and proof correction. The final published version may differ from this proof.

TI-RADS level			0.059
TR 4	79 (54)	37 (41)	
TR 5	68 (46)	53 (59)	
Composition			0.857
Solid	138 (94)	85 (94)	
Mixed cystic and solid	9 (6)	5 (6)	
Hashimoto thyroiditis			0.127
Positive	12 (8.2)	13 (14.4)	
†Negative	135 (91.8)	77 (85.6)	
Nodular goiter			0.014
Positive	31 (21.1)	1 (2.2)	
Negative	116 (78.9)	44 (97.8)	
BMUS Rad-score, median (interquartile range)	-0.38 (-0.49 to -0.30)	-0.37 (-0.45 to -0.24)	0.206
SWE Rad-score, median (interquartile range)	0.07 (-0.68 to 0.54)	-0.15 (-0.84 to 0.37)	0.249

Abbreviations: US, ultrasound; LN, lymph node; TI-RADS: Thyroid Imaging, Reporting and Data System; BMUS, B-model ultrasound; SWE, shear-wave elastography; Rad-score, radiomics score. Data are number of patients and percentage if not specified.

*Multifocality refers to more than one tumor site in the thyroid, which was evaluated by preoperative biopsy and confirmed by pathological examination of resection specimens.

† Determined based on pathology.

Table 2. Pathological characteristics of study cohort.

	Training cohort (n = 147)	Validation cohort (n = 90)
Pathologic T stage, No. (%)		
pT1	114 (78%)	80 (89%)
pT2	22 (15%)	6 (7%)
pT3	2 (1%)	3 (3%)
pT4	9 (6%)	1 (1%)
Pathologic N stage, No. (%)		
pN0	72 (49%)	52 (58%)
pN1a	48 (33%)	24 (27%)
pN1b	27 (18%)	14 (15%)
Number of LNs removed		
Central		
Median (interquartile range)	9 (5-13)	7 (5-8)
Lateral		
†Median (interquartile range)	17 (6-23)	17 (3-21)
Number of positive LNs		
Central		
†Median (interquartile range)	5 (3-8)	4 (3-7)
Lateral		
Median (interquartile range)	4 (2-7)	3 (2-6)

Abbreviation: LNs, lymph nodes.

† Bilateral.

Thyroid
Nomogram based on shear-wave elastography radiomics can improve preoperative cervical lymph node staging for papillary thyroid carcinoma (DOI: 10.1089/thy.2019.0780)
This paper has been peer-reviewed and accepted for publication, but has yet to undergo copyediting and proof correction. The final published version may differ from this proof.

Table 3. Demographic and clinicopathological characteristics of patients by lymph node status.

Thyroid
Nomogram based on shear-wave elastography radiomics can improve preoperative cervical lymph node staging for papillary thyroid carcinoma (DOI: 10.1089/thy.2019.0780)

Characteristic	Training cohort No. (%)			Validation cohort No. (%)		
	LN metastasis (+)	LN metastasis (-)	P value	LN metastasis (+)	LN metastasis (-)	P value
Age (Mean ± SD, years)	41.32 ± 10.18	41.86 ± 9.19	0.736	39.50± 10.33	45.81 ± 10.38	0.005
Age (years)			0.384			0.194
>55	7 (9.3)	4 (5.6)		3 (7.9)	9 (17.3)	
≤55	68 (90.7)	68 (94.4)		35 (92.1)	43 (82.7)	
Age (years)			0.383			0.004
>45	24 (32.0)	28 (38.9)		9 (18.2)	28 (58.8)	
≤45	51 (68.0)	44 (61.1)		29 (81.8)	24 (41.2)	
Gender			0.095			0.018
Male	26 (34.7)	16 (22.2)		11 (28.9)	5 (9.6)	
Female	49 (65.3	56 (77.8)		27 (71.1)	47 (90.4)	
Primary site			0.138			0.729
Right lobe	34 (45.3)	35 (48.6)		18 (47.4)	29 (55.8)	
Left lobe	37 (49.3)	37 (51.4)		19 (50.0)	22 (42.3)	
Isthmus	4 (5.3)	0 (0.0)		1 (2.6)	1 (1.9)	
Tumor location			0.073			0.143
Sub-capsular	37 (49.3)	25 (34.7)		19 (50.0)	18 (34.6)	
Intra-thyroidal	38 (50.7)	47 (65.3)		19 (50.0)	34 (65.4)	
Tumor size, mean ± SD, mm	15.15 ± 7.95	9.65 ± 5.59	<0.001	13.82 ± 6.91	10.06 ± 4.16	0.004
Multifocality			0.008			0.114
Positive	23 (30.7)	9 (12.5)		12 (31.6)	9 (17.3)	
Negative	52 (69.3)	63 (87.5)		26 (68.4)	43 (82.7)	

US-reported LN status			<0.001			0.019
Positive	28 (37.3)	4 (5.6)		9 (81.8)	14 (41.2)	
Negative	47 (62.7)	68 (94.4)		2 (18.2)	20 (58.8)	
TI-RADS level			0.117			0.255
TR 4	38 (48.1)	24 (35.3)		13	24	
TR 5	41 (51.9)	44 (64.7)		25	28	
Composition			0.097			0.078
Solid	68 (90.7)	70 (97.2)		34 (89.5)	51 (98.1)	
Mixed cystic and solid	7 (9.3)	2 (2.8)		4 (10.5)	1 (1.9)	
Hashimoto thyroiditis			0.597			0.366
Positive	7 (9.3)	5 (6.9)		4 (10.5)	9 (17.3)	
Negative	68 (90.7)	67 (93.1)		34 (89.5)	43 (82.7)	
Nodular goiter			0.632			0.019
Positive	17 (22.7)	14 (19.4)		7 (18.4)	1 (1.9)	
Negative	58 (77.3)	58 (80.6)		31 (81.6)	51 (98.1)	
BMUS rad-score, median (interquartile range)	0.16 (0.02 to 0.30)	-0.04 (-0.21 to 0.08)	<0.001	-0.25 (-0.38 to 0.13)	-0.41 (-0.47 to -0.29)	<0.001
SWE rad-score, median (interquartile range)	0.49 (0 to 0.97)	-0.50 (-1.35 to 0.19)	<0.001	0.26 (-0.29 to 0.80)	-0.51 (-0.38 to 0.08)	<0.001

Abbreviations: LN, lymph node; US, ultrasound; TI-RADS: Thyroid Imaging, Reporting and Data System; BMUS, B-model ultrasound; SWE, shear-wave elastography; Rad-score, radiomics score.

Thyroid
Nomogram based on shear-wave elastography radiomics can improve preoperative cervical lymph node staging for papillary thyroid carcinoma (DOI: 10.1089/thy.2019.0780)
This paper has been peer-reviewed and accepted for publication, but has yet to undergo copyediting and proof correction. The final published version may differ from this proof.

Table 4. Risk factors for cervical lymph node metastasis based on preoperative data in the training cohort.

		Clinical model			SWE radiomics nomogram	
Intercept and variable	β	Odds ratio (95% CI)	P value	β	Odds ratio (95% CI)	P value
Intercept	-1.943			-0.550		
Tumor size	0.113	1.119 (1.051 to 1.192)	<0.001	NA	NA	NA
Multifocality	1.330	3.780 (1.446 to 9.883)	0.007	1.446	4.245 (1.386 to 13.003)	0.011
US-reported LN status	2.058	7.831 (2.437 to 25.167)	0.001	1.469	4.344 (1.235 to 15.286)	0.022
BMUS Rad-score	NA	NA	NA	NA	NA	NA
SWE Rad-score	NA	NA	NA	1.372	3.943 (2.258 to 6.884)	<0.001
AUC						*P value
Training cohort	0.800 (0.729 to 0.871)			0.851 (0.791 to 0.912)		0.034
Validation cohort	0.783 (0.689 to 0.876)			0.832 (0.749 to 0.916)		0.048

Abbreviations: PTC, papillary thyroid carcinoma; US, ultrasound; BMUS, B-model ultrasound; SWE, shear-wave elastography; NA, not available; Rad-score, radiomics score.

*P value represents difference of AUC between SWE radiomics nomogram and clinical model.

Thyroid
Nomogram based on shear-wave elastography radiomics can improve preoperative cervical lymph node staging for papillary thyroid carcinoma (DOI: 10.1089/thy.2019.0780)
This paper has been peer-reviewed and accepted for publication, but has yet to undergo copyediting and proof correction. The final published version may differ from this proof.

Table 5. Evaluation of the SWE radiomics signature with respect to NRI and IDI.

Characteristic	Training cohort			Validation cohort		
	Categorical NRI (95% CI)	Continuous NRI (95% CI)	IDI (95% CI)	Categorical NRI (95% CI)	Continuous NRI (95% CI)	IDI (95% CI)
SWE radiomics nomogram vs. clinical model	0.547 (0.332 to 0.762)	0.607 (0.301 to 0.912)	0.103 (0.054 to 0.151)	0.443 (0.147 to 0.39)	0.666 (0.279 to 1.053)	0.145 (0.068 to 0.222)
P value	<0.0001	<0.0001	<0.0001	0.0034	0.0007	0.0002

Abbreviations: SWE, shear-wave elastography; NRI, net reclassification improvement; IDI, index integrated discrimination improvement.

Thyroid
Nomogram based on shear-wave elastography radiomics can improve preoperative cervical lymph node staging for papillary thyroid carcinoma (DOI: 10.1089/thy.2019.0780)
This paper has been peer-reviewed and accepted for publication, but has yet to undergo copyediting and proof correction. The final published version may differ from this proof.

Table 6. Performance of the prediction Nomo-score for estimating the risk of lymph node metastasis.

	Value (95% CI)		
Variable	Training Cohort (147)	Validation Cohort (90)	Combined cohort (237)
Cutoff value	0.574	0.574	0.574
AUC	0.851 (0.791 to 0.912)	0.832 (0.749 to 0.916)	0.839 (0.789 to 0.889)
Sensitivity, %	80.67 (69.56 to 89.76)	86.84 (72.67 to 94.25)	84.34 (75.58 to 91.50)
Specificity, %	87.50 (77.92 to 93.28)	73.08 (59.75 to 83.23)	82.26 (74.60 to 87.98)
Positive predictive value, %	85.48 (74.66 to 92.17)	70.21 (56.02 to 81.35)	79.25 (70.57 to 85.88)
Negative predictive value, %	74.12 (63.91 to 82.24)	88.37 (75.52 to 94.93)	77.86 (70.02 to 84.12)
Positive likelihood ratio	5.65 (4.48 to 7.14)	3.23 (2.78 to 3.74)	4.19 (3.80 to 4.62)
Negative likelihood ratio	0.34 (0.31 to 0.37)	0.18 (0.12 to 0.27)	0.31 (0.29 to 0.34)
Diagnostic Accuracy, %	78.91 (71.62 to 84.73)	78.89 (69.37 to 86.05)	78.48 (72.82 to 83.24)

Thyroid
elastography radiomics can improve preoperative cervical lymph node staging for papillary thyroid carcinoma (DOI: 10.1089/thy.2019.0780)
d and accepted for publication, but has yet to undergo copyediting and proof correction. The final published version may differ from this proof.

Figure legends

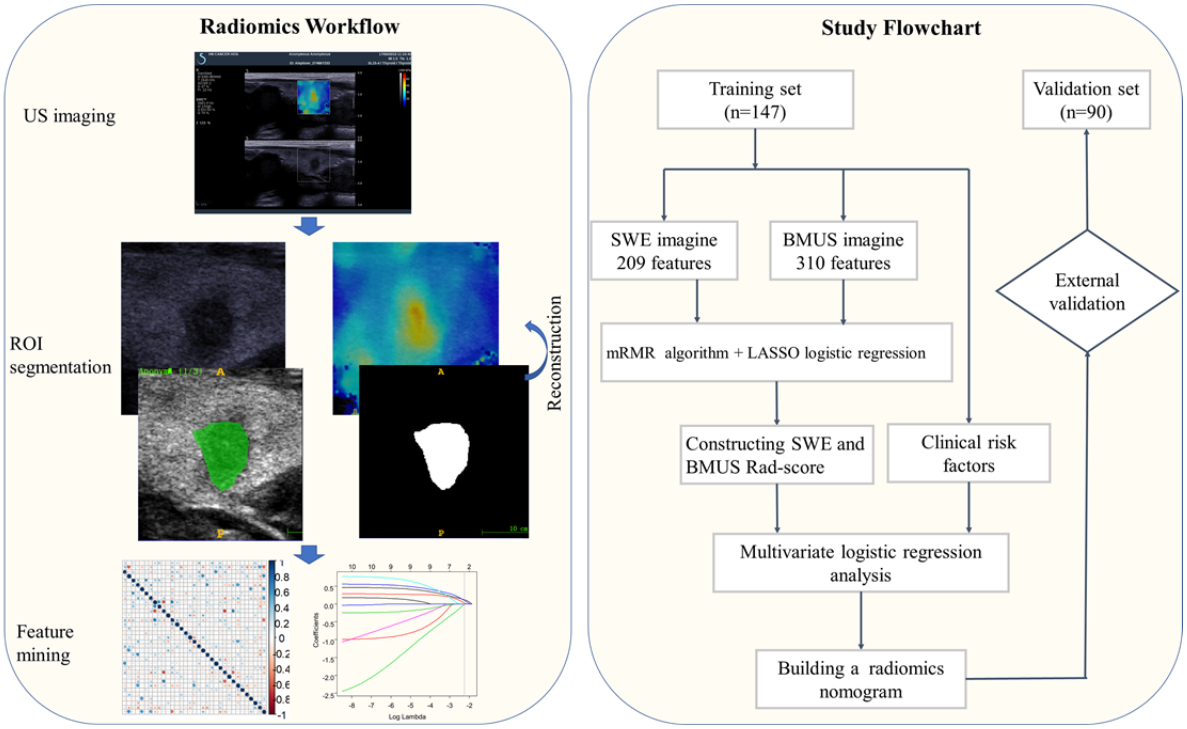

Figure 1 Ultrasound radiomics workflow and study flowchart. Abbreviations: US, ultrasound; ROI, region of interest; BMUS, B-model ultrasound; SWE, shear-wave elastography; mRMR, minimum redundancy maximum relevance; LASSO, least absolute shrinkage and selection operator.

Thyroid
Nomogram based on shear-wave elastography radiomics can improve preoperative cervical lymph node staging for papillary thyroid carcinoma (DOI: 10.1089/thy.2019.0780)
This paper has been peer-reviewed and accepted for publication, but has yet to undergo copyediting and proof correction. The final published version may differ from this proof.

Thyroid
Nomogram based on shear-wave elastography radiomics can improve preoperative cervical lymph node staging for papillary thyroid carcinoma (DOI: 10.1089/thy.2019.0780)

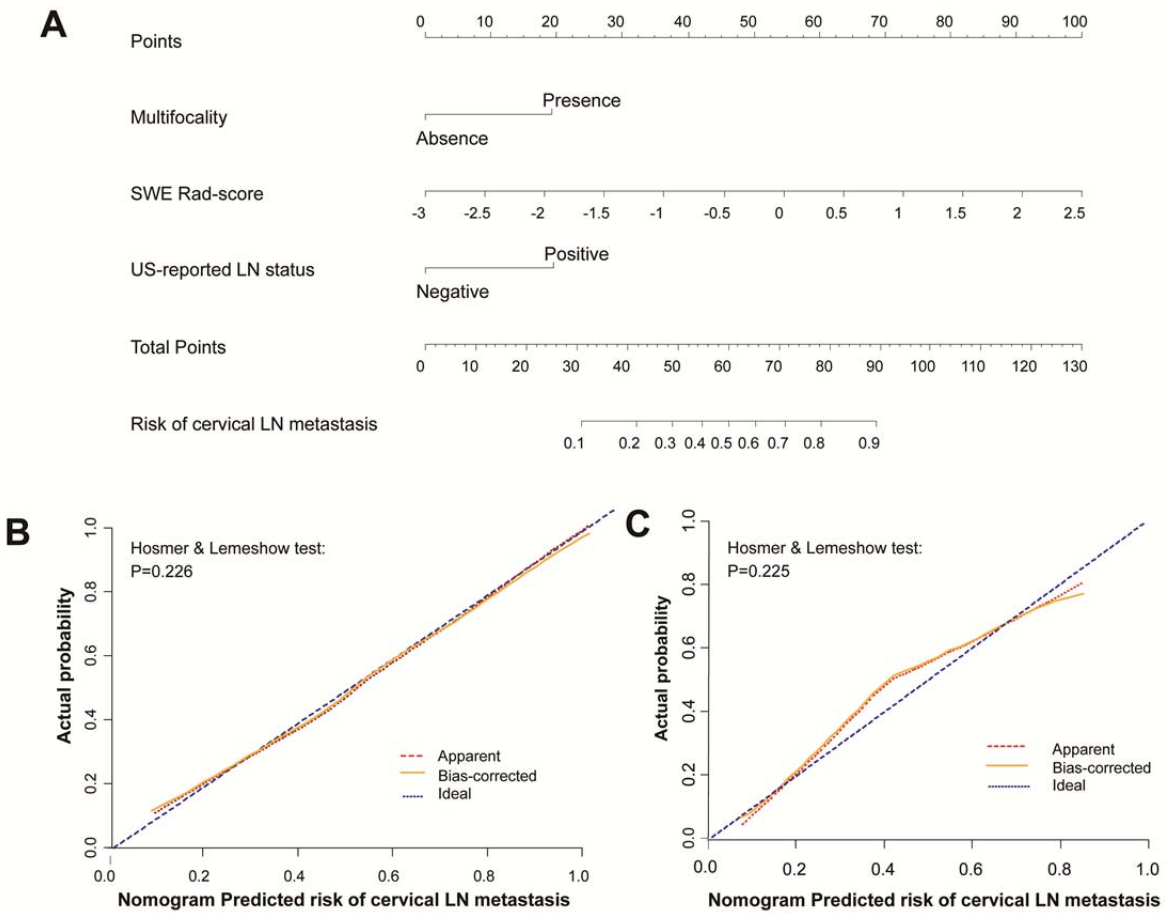

Figure 2 SWE radiomics nomogram for the preoperative estimation of cervical LN metastasis. (A) Nomogram to estimate the risk of LN metastasis preoperatively in papillary thyroid carcinoma. To use the nomogram, find the position of each variable on the corresponding axis, draw a vertical line to the points axis for the number of points, add the points from all of the variables, and draw a line from the total points axis to determine the LN metastasis probabilities at the lower line of the nomogram. (B) and (C) Calibration curves of the SWE radiomics nomogram in the training (B) and validation (C) set. Calibration curves depict the calibration of SWE radiomics model in terms of the agreement between the predicted probabilities of LN metastasis and observed outcomes of LN metastasis. The dotted blue line represents an ideal prediction, and the dotted red line represents the predictive ability of the nomogram. The closer the dotted red line fit is to the dotted blue line, the better the predictive accuracy of the nomogram is.

Thyroid
Nomogram based on shear-wave elastography radiomics can improve preoperative cervical lymph node staging for papillary thyroid carcinoma (DOI: 10.1089/thy.2019.0780)

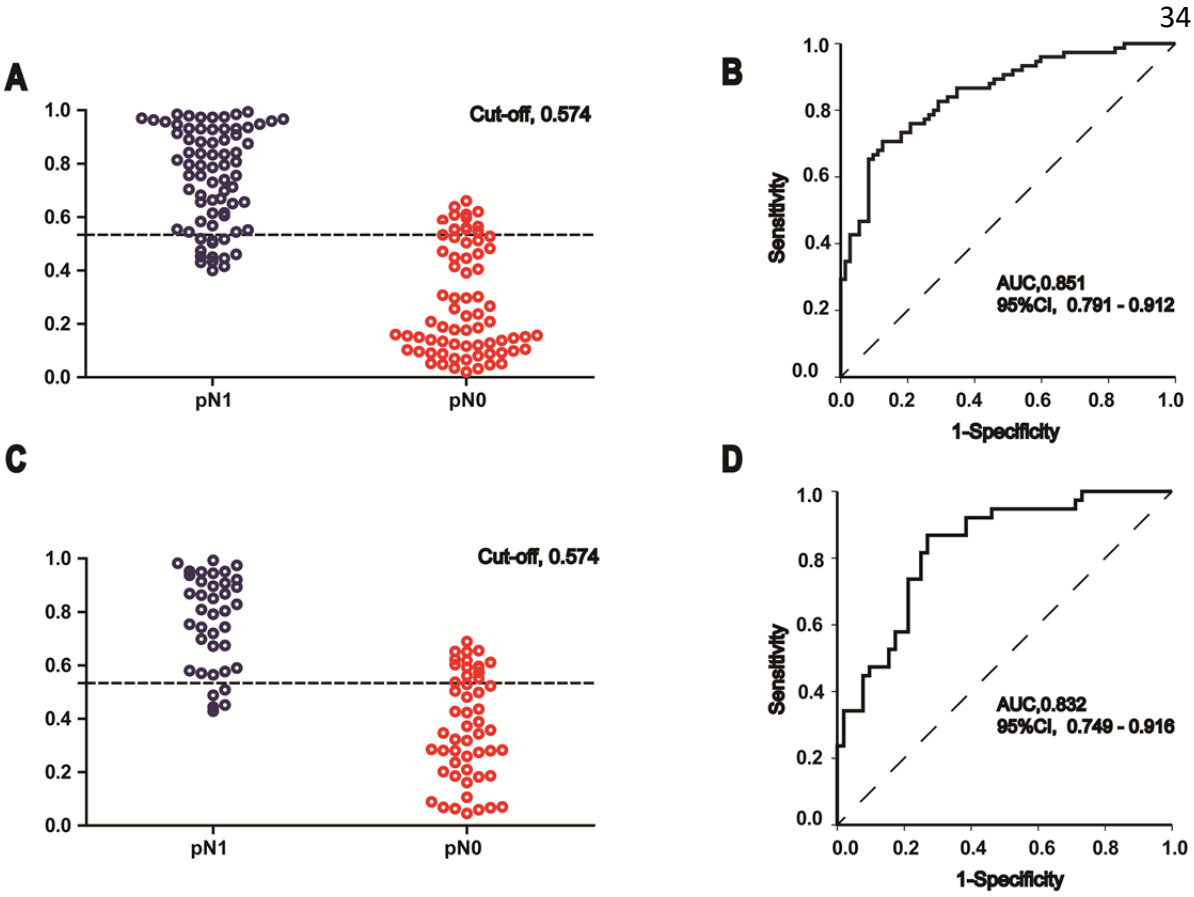

Figure 3 Diagnostic accuracy of the SWE radiomics nomogram for the estimation of LN metastasis in patients with papillary thyroid carcinoma in the training and validation cohort. In panel (A) and (C), the use of a cut-off value of 0.574 of the Nom-score performed well for the differential diagnosis of pN1 from pN0 in the training (A) and validation (C) cohort. In panel (B) and (D), ROC curves show good diagnostic performance of the nomogram in the training and validation cohort.

Thyroid
Nomogram based on shear-wave elastography radiomics can improve preoperative cervical lymph node staging for papillary thyroid carcinoma (DOI: 10.1089/thy.2019.0780)
This paper has been peer-reviewed and accepted for publication, but has yet to undergo copyediting and proof correction. The final published version may differ from this proof.

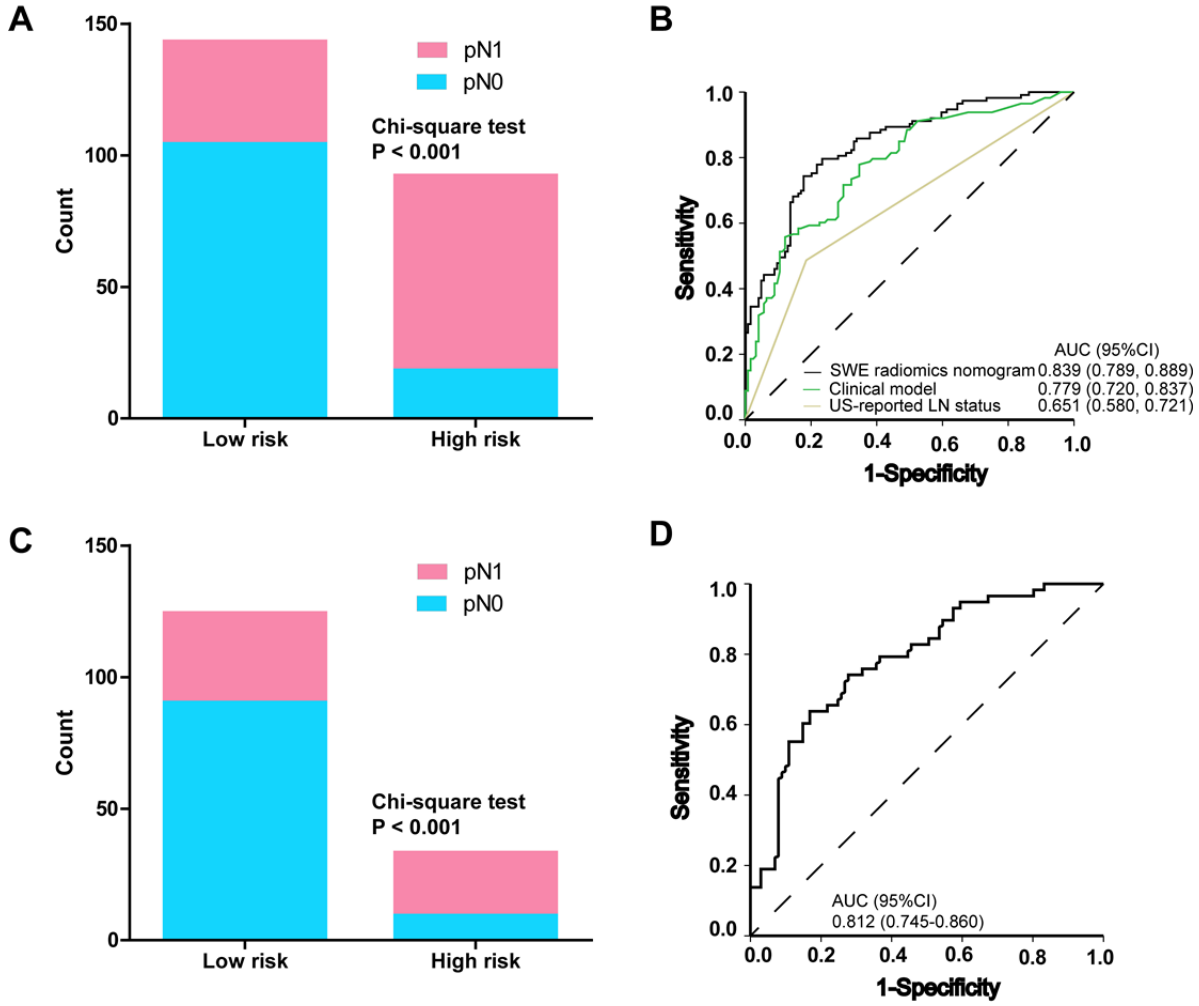

Figure 4 Performance of the nomogram in all 237 patients and in the cN0 subgroup (n =159). The left panels show the risk-classification performance of the nomogram. The right panels present the ROC curve analyses for the nomogram. (A, B) All 237 patients. (C, D) cN0 subgroup.

Appendix Table A1 Major packages of R software used in this study.

Functions	R package
LASSO regression	glmnet
mRMR algorithm	mRMRe
Univariate logistic regression analysis	glm
Plot the receiver operating curve (ROC) and measure the area under the ROC (AUC)	pROC
For ROC analysis to determine optimal cutoff value	OptimalCutpoints
Plot bar diagrams	ggplot2
Plot calibration curves	rms
Decision curve analysis (DCA)	rmda

Thyroid
Nomogram based on shear-wave elastography radiomics can improve preoperative cervical lymph node staging for papillary thyroid carcinoma (DOI: 10.1089/thy.2019.0780)
This paper has been peer-reviewed and accepted for publication, but has yet to undergo copyediting and proof correction. The final published version may differ from this proof.

Appendix Figure A1:

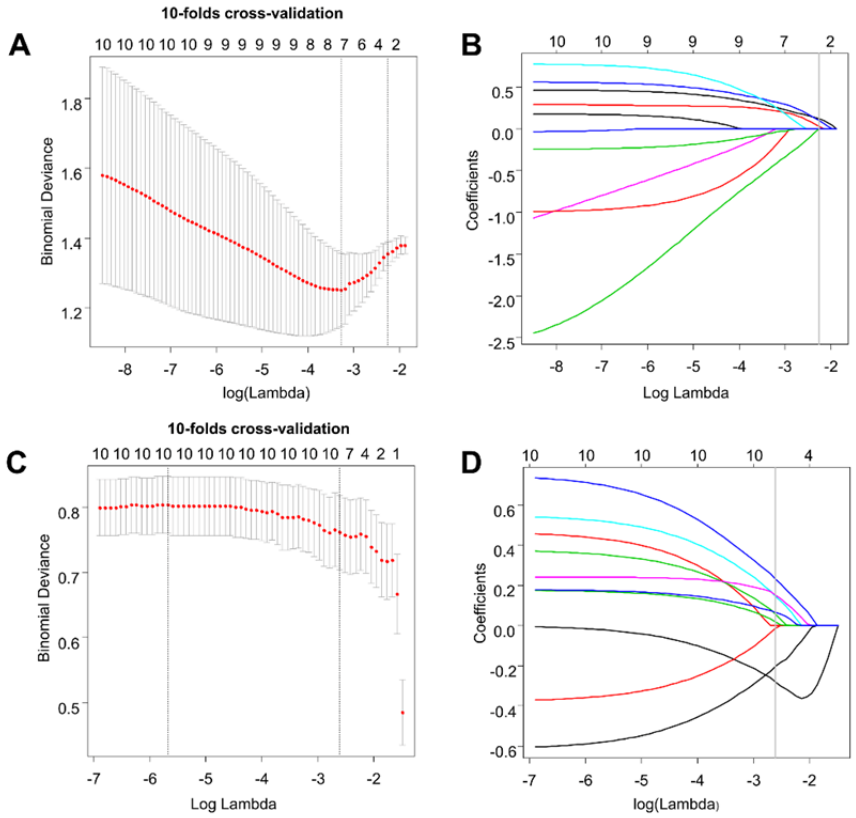

Appendix Figure A1 Ultrasound image feature selection using the least absolute shrinkage and selection operator (LASSO) logistic regression model in the training cohort. (A) and (C) The 10-fold cross-validation and the minimal criteria process was used to generate the optimal penalization coefficient lambda (λ) in the LASSO model. As a result, λ values of -1.858138 and -1.861558 were selected for the BMUS (A) and SWE (C) features, respectively. (B) and (D) LASSO coefficient profiles of the BMUS and SWE features. The dotted vertical line was drawn at the value selected by 10-fold cross-validation when the optimal λ resulted in two (BMUS) and four (SWE) nonzero coefficients, respectively.

Thyroid
Nomogram based on shear-wave elastography radiomics can improve preoperative cervical lymph node staging for papillary thyroid carcinoma (DOI: 10.1089/thy.2019.0780)
This paper has been peer-reviewed and accepted for publication, but has yet to undergo copyediting and proof correction. The final published version may differ from this proof.

Appendix Figure A2:

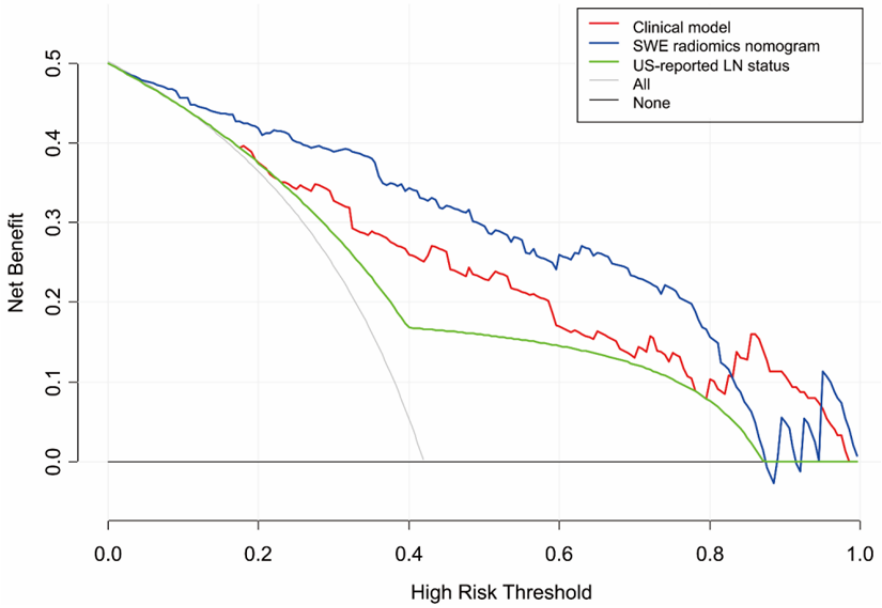

Appendix Figure A2 Decision curve analysis (DCA) of each model in predicting LN metastasis for papillary thyroid carcinoma. The vertical axis measures standardized net benefit. The horizontal axis shows the corresponding risk threshold. The DCA showed that if the threshold probability is between 0 and 0.83, using the SWE radiomics nomogram (blue curve) derived in the present study to predict LN metastasis provided a greater benefit than the clinical model (red curve) and US-reported LN status alone (green curve).

Thyroid
Nomogram based on shear-wave elastography radiomics can improve preoperative cervical lymph node staging for papillary thyroid carcinoma (DOI: 10.1089/thy.2019.0780)
This paper has been peer-reviewed and accepted for publication, but has yet to undergo copyediting and proof correction. The final published version may differ from this proof.

Appendix A1 Detailed descriptions on shear-wave elastography (SWE).

SWE is currently under evaluation for thyroid cancer detection, utilizing the fact that malignancies are generally stiffer than benign lesions. SWE was conducted for the suspicious thyroid nodules on B-model ultrasound (BMUS). It was performed in dual mode, i.e. elastograms displayed alongside BMUS in real-time and using default elasticity settings of acoustic impulse intensity, smoothing, persistence, and kPa display scale (0-180 kPa; measurements were independent of the selected display maximum). In this regard, blue and red areas on elastograms corresponded to comparatively low kPa (soft) and high kPa (stiff) regions, respectively (1,2). On the SWE display, an electronic window was selected that included the whole region of the lesion. Three or more SWE/US cineloop segments lasting 10 s each were acquired through different parts of the lesion, each time keeping the transducer completely stationery during captures. The operator then replayed the cineloops, disregarding the first few seconds as the elastograms had not stabilized, and selected single static images that were deemed to be temporally stable and containing the fewest artifacts, such as vertical linear bands of color crossing different tissues or other high stiffness color regions in the surrounding fascia (1). For each selected static image, the region of interest was set to include the whole thyroid lesion and adjacent normal parenchyma. Besides, the stiffest region in the lesion was selected by visual inspection, onto which a Q-Box measured 1 or 2 mm in diameter was placed. The software generated several indices for each Q-Box, of which mean (E_{mean}), minimum (E_{min}) and maximum (E_{max}) elasticity values (kPa) were recorded (**Fig. S1**). We also measured the elasticity index of the adjacent normal parenchyma to obtain a ratio (E_{mean-m}) of the E_{mean} of thyroid nodules and E_{mean} of adjacent normal parenchyma.

Thyroid
Nomogram based on shear-wave elastography radiomics can improve preoperative cervical lymph node staging for papillary thyroid carcinoma (DOI: 10.1089/thy.2019.0780)
This paper has been peer-reviewed and accepted for publication, but has yet to undergo copyediting and proof correction. The final published version may differ from this proof.

Thyroid

Nomogram based on shear-wave elastography radiomics can improve preoperative cervical lymph node staging for papillary thyroid carcinoma (DOI: 10.1089/thy.2019.0780)

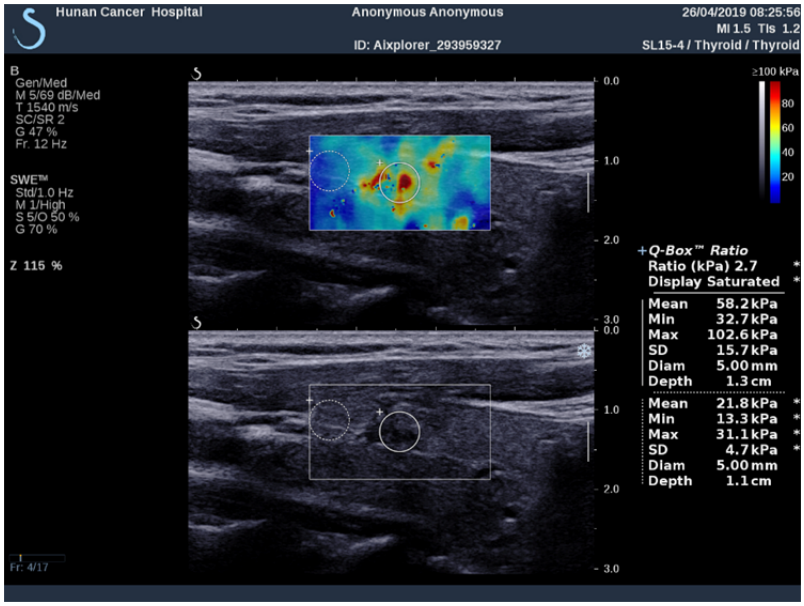

Fig.S1 A 47-year-old woman with papillary thyroid carcinoma (PTC) and negative cervical lymph node (LN) metastasis. The BMUS image shows a 15-mm-size hypoechoic mass with macrocalcifications in the right lobe of the thyroid gland, diagnosed as PTC via US-guided fine-needle aspiration biopsy and confirmed by the pathological examination after surgery. The preoperative BMUS showed no suspicious cervical LNs. On SWE, the region of interest was placed on the entire region of the lesion (white square area) and adjacent normal parenchyma. A 2-mm-sized circular region of interest (Q-Box) was selected at the stiffest portion and elasticity scores of 58.2 kPa (E_{mean}), 102.6 kPa (E_{max}), 32.7 kPa (E_{min}), and 2.7 ($E_{mean\text{-}m}$) were obtained. The patient underwent total thyroidectomy with central neck node dissection, and pathology showed no cervical LN metastasis.

References:

1. Bhatia KS, Cho CC, Tong CS, Yuen EH, Ahuja AT 2012 Shear wave elasticity imaging of cervical lymph nodes. Ultrasound Med Biol **38**:195-201.

2. Park YJ, Kim JA, Son EJ, Youk JH, Park CS 2013 Quantitative shear wave elastography as a prognostic implication of papillary thyroid carcinoma (PTC): elasticity index can predict extrathyroidal extension (ETE). Ann Surg Oncol **20**:2765-2771.

Appendix A2 Detailed descriptions of the statistical methodology.

Thyroid
Nomogram based on shear-wave elastography radiomics can improve preoperative cervical lymph node staging for papillary thyroid carcinoma (DOI: 10.1089/thy.2019.0780)

Ⅰ. The least absolute shrinkage and selection operator (LASSO) algorithm

We used the LASSO algorithm to select the most important LN-status related features and construct radiomics signature for BMUS and SWE in the training set. This algorithm minimizes a log partial likelihood subject to the sum of the absolute values of the parameters bounded by a constant:

$$\hat{\beta} = \arg\min \ell(\beta), \text{subject to} \sum |\beta_j| \leq t$$

where $\hat{\beta}$ is the obtained parameters, $\ell(\beta)$ is the log partial likelihood of the logistic regression model, and $t > 0$ is a constant.

The LASSO algorithm shrinks some coefficients and reduces others to exactly 0 via the absolute constraint. In this study, the constant *t* was set as 0.015, and LASSO selected 2 and 4 nonzero coefficients $\hat{\beta}$ for BMUS and SWE, respectively.

Reference: Sauerbrei W, Royston P, Binder H 2007 Selection of important variables and determination of functional form for continuous predictors in multivariable model building. Stat Med **26**:5512-5528.

Ⅱ. Decision curve analysis (DCA)

The DCA was used to assess the clinical utility of the SWE radiomics nomogram. The DCA algorithm assesses prediction models by calculating the range of threshold probabilities in which a prediction model was clinically useful. DCA is a compositive method for evaluating and comparing different prediction models. The theory of DCA can be illustrated by the equation below:

$$\frac{a-c}{d-b} = \frac{1-P_t}{P_t}$$

where $d - b$ represents the influence of unnecessary treatment. If treatment is directed by a prediction model, $d - b$ is the harm related to a false-positive result compared with a true-negative result. Inversely, $a - c$ represents the consequence of rejecting beneficial treatment, in other words, the harm from a false-negative result compared with a true-positive result. P_t represents where the expected benefit of treatment is equal to the expected benefit of refraining from treatment.

Reference: Vickers AJ, Elkin EB 2006 Decision curve analysis: a novel method for evaluating prediction models. Med Decis Making **26**:565-574.

Appendix A3 Radiomics score formula.

BMUS radiomics score = 0.058013558635542 + 0.105558730672956*
original_shape2D_Perimeter + 0.0389437259845566*
wavelet.LH_glszm_ZoneEntropy

SWE radiomics score = 0.0413235734632436 + 0.132584455613722*
logarithm_glszm_ZoneEntropy_R - 0.0447489903756448*
gradient_glcm_Imc1_B - 0.059741932538859*
wavelet.LH_glszm_SmallAreaLowGrayLevelEmphasis_GREY -
0.0319998073308202* wavelet.LH_ngtdm_Contrast_G

Thyroid
Nomogram based on shear-wave elastography radiomics can improve preoperative cervical lymph node staging for papillary thyroid carcinoma (DOI: 10.1089/thy.2019.0780)
This paper has been peer-reviewed and accepted for publication, but has yet to undergo copyediting and proof correction. The final published version may differ from this proof.